Intramolecular interactions control Vms1 translocation to damaged mitochondria

Jin-Mi Heo[a,*], Jason R. Nielson[a], Noah Dephoure[b], Steven P. Gygi[b], and Jared Rutter[a]
[a]Department of Biochemistry, University of Utah School of Medicine, Salt Lake City, UT 84132; [b]Department of Cell Biology, Harvard Medical School, Boston, MA 02115

ABSTRACT **Mitochondrial dysfunction is associated with the development of many age-related human diseases. Therefore recognizing and correcting the early signs of malfunctioning mitochondria is of critical importance for cellular welfare and survival. We previously demonstrated that VCP/Cdc48-associated mitochondrial stress responsive 1 (Vms1) is a component of a mitochondrial surveillance system that mediates the stress-responsive degradation of mitochondrial proteins by the proteasome. Here we propose novel mechanisms through which Vms1 monitors the status of mitochondria and is recruited to damaged or stressed mitochondria. We find that Vms1 contains a highly conserved region that is necessary and sufficient for mitochondrial targeting (the mitochondrial targeting domain [MTD]). Of interest, MTD-mediated mitochondrial targeting of Vms1 is negatively regulated by a direct interaction with the Vms1 N-terminus. Using laser-induced generation of mitochondrial reactive oxygen species, we also show that Vms1 is preferentially recruited to mitochondria subjected to oxidative stress. These studies define cellular and biochemical mechanisms by which Vms1 localization to mitochondria is controlled to enable an efficient protein quality control system.**

Monitoring Editor
Thomas D. Fox
Cornell University

Received: Feb 4, 2013
Revised: Feb 22, 2013
Accepted: Feb 26, 2013

INTRODUCTION

Mitochondria are involved in many essential cellular processes, including ATP generation, heme biosynthesis, apoptosis, and amino acid/fatty acid metabolism (Calvo and Mootha, 2010). Mitochondrial impairment therefore is associated with the development of a broad spectrum of human diseases, from diabetes, heart failure, and cancer to neurodegenerative diseases (Lin and Beal, 2006). Accordingly, maintenance of mitochondrial function is of critical importance to avoid a variety of human pathologies.

Previously we showed that VCP/Cdc48-associated mitochondrial stress responsive 1 (Vms1) promotes stress-responsive mitochondrial protein degradation by the ubiquitin/proteasome system (UPS) in yeast (Lin and Beal, 2006). Although it is cytoplasmic in normal conditions, Vms1 translocates to mitochondria in response to a variety of mitochondrial stressors (Heo *et al.*, 2010; Tanaka *et al.*, 2010). Vms1 also promotes the recruitment of the UPS components Cdc48 and Npl4 to the mitochondria, where they facilitate proteasomal protein degradation. The mammalian orthologue of Cdc48, known as VCP or p97, translocates to ubiquitinated mitochondria and mediates the degradation of ubiquitinated mitochondrial proteins (e.g., Mfn1/2 and Mcl1) by the proteasome (Tanaka *et al.*, 2010; Chan *et al.*, 2011; Xu *et al.*, 2011). Moreover, increasing numbers of mitochondrial proteins located in each of the different mitochondrial compartments have been demonstrated to be targets of proteasomal degradation (Heo and Rutter, 2011; Livnat-Levanon and Glickman, 2011). Mitochondrial proteins are clearly targeted for UPS-mediated degradation, and the maintenance of mitochondrial function appears to rely on this protein degradation activity.

Identification of Vms1 and its function, in addition to providing insight into the mechanisms of mitochondrial protein degradation, has also raised a number of questions that remain to be addressed. Among them, we have focused on determining the underlying mechanism(s) by which the intracellular localization of Vms1 is regulated. Here we propose mechanisms by which the localization of

This article was published online ahead of print in MBoC in Press (http://www.molbiolcell.org/cgi/doi/10.1091/mbc.E13-02-0072) on March 6, 2013.

*Present address: Department of Cell Biology, Harvard Medical School, Boston, MA 02115.

Address correspondence to: Jared Rutter (rutter@biochem.utah.edu).

Abbreviations used: MTD, mitochondrial targeting domain; PMS, postmitochondrial supernatant; UPS, ubiquitin-proteasome system; VIM, VCP-interacting motif; WCE, whole cell extract.

Vms1 is regulated. We find that an internal highly conserved region of Vms1, which we name the mitochondrial targeting domain (MTD), is necessary and sufficient for mitochondrial localization of the protein. Of interest, our data suggest that the Vms1 N-terminus negatively regulates mitochondrial localization via a direct interaction. We propose that dissociation of this interaction upon mitochondrial stress promotes the mitochondrial translocation of Vms1. These observations made it imperative to understand the nature and location of the "mitochondrial stress" signal. Does the presence of mitochondrial stress in the cell promote a generalized response in which Vms1 translocates to all mitochondria nonspecifically? Alternatively, is the damaged subpopulation of mitochondria selectively marked, thereby enabling Vms1 to localize specifically to these mitochondria? Our results demonstrate that focal oxidative damage induces specific mitochondrial localization, suggesting the marking of damaged mitochondria. Combining these data, we propose a two-step model in which stressed mitochondria present or activate a "receptor" specifically on the outer membrane of damaged mitochondria, which promotes the local dissociation of the Vms1 N-terminus/MTD interaction. The MTD is then free to mediate the stable localization of Vms1 and its associated proteins to mitochondria. Taken together, the results of this study provide insight into the mechanisms by which damaged mitochondria communicate with the rest of the cell to promote an effective stress response to maintain mitochondrial, cellular, and organismal viability.

RESULTS

Regulated mitochondrial localization of Vms1

Proteomics studies of yeast mitochondria suggested that Vms1 is found in purified mitochondria (Sickmann *et al.,* 2003). As a result, we were surprised to observe almost exclusively cytoplasmic localization of a fully functional Vms1–green fluorescent protein (GFP) fusion (Heo *et al.,* 2010). However, in cells treated with mitochondrial stress inducers, Vms1-GFP localized to mitochondria in all cells (Heo *et al.,* 2010).

The Vms1 protein contains three recognizable regions. The N-terminus contains a C2H2-type zinc finger domain (ZnF). The C-terminus contains an ankyrin repeat and predicted coiled-coil (CC), followed by the VCP interacting motif (VIM), which is responsible for VCP/Cdc48 interaction. Between these domains is a highly conserved region of unknown structure (residues 182–417), which we named the MTD (Figure 1A). To determine which of these regions is required for mitochondrial localization, we generated a series of N- and C-terminal deletion mutants (Figure 1A). As shown in Figure 1B, the wild-type protein was cytoplasmic in normal conditions but translocated to mitochondria upon treatment with rapamycin, which causes mitochondrial stress (Kissová *et al.* 2006; Heo *et al.,* 2010; Pan, 2011). Deletion of the N-terminus (mutant 182-end), however, caused localization to mitochondria both in the presence and absence of rapamycin. Deletion of the C-terminal ankyrin repeat, coiled-coil, and VIM (mutant 1-417) had no effect on localization (Figure 1B). Deletion of the middle MTD region from either the N- or C-terminus resulted in a complete loss of mitochondrial localization even in the presence of rapamycin (mutants 417-end and 1-182). An N- and C-terminal truncation containing only the MTD constitutively localized to mitochondria (mutant 182-417). These data suggest that the MTD is necessary and sufficient for the mitochondrial localization of Vms1 (Supplemental Figure S1), which is repressed in-*cis* by the N-terminus.

The constitutive mitochondrial localization of the isolated MTD was verified by biochemical fractionation. In normal conditions, wild-type Vms1 was present in the whole-cell extract (WCE) and postmitochondrial supernatant (PMS) but was largely absent from both the crude and highly purified mitochondrial fractions (Figure 1C). The MTD-only Vms1 protein, however, was depleted from the PMS fraction and was found predominantly in the mitochondrial fractions (Figure 1C). The interaction between the MTD and mitochondria appears to be fairly stable due to its persistence through the multistep mitochondrial purification procedure.

Unlike the 182-417 mutant, the 1-417 mutant containing both the N-terminus and MTD exhibited a wild-type localization pattern. It was observed to have cytoplasmic localization until treatment with rapamycin (Figure 1B). This implies that the N-terminus negatively regulates the MTD-mediated mitochondrial targeting of Vms1 in normal conditions. On mitochondrial stress, however, this suppression is removed and Vms1 relocalized to the mitochondria.

We assayed each of these five deletion mutants for complementation of the *vms1*Δ rapamycin hypersensitivity phenotype and found that none of them can replace *VMS1* function in vivo (Supplemental Figure S2A). We showed previously that mitochondrial recruitment of Cdc48 and Npl4 is an essential Vms1 function, and this interaction is formed through the highly conserved VIM located near the extreme C-terminus of Vms1 (Heo *et al.,* 2010). Mutants 1-182, 1-417, and 182-417 lack this VIM sequence and therefore fail to recruit Cdc48 and Npl4 to mitochondria. As a result, these variants are incompetent to restore Vms1 function. Although the 417-end mutant can form a stronger interaction with both Cdc48 and Npl4 than can the full-length Vms1 (Heo *et al.,* 2010), loss of the MTD prevents its mitochondrial targeting even in the presence of stress stimuli, thus abolishing function. Finally, the 182-end mutant containing both the MTD and VIM could not rescue the *vms1*Δ mutant phenotype either. For an unknown reason, this 182-end mutant does not form a stable interaction with Cdc48 and Npl4 (Supplemental Figure S2B). From our ongoing efforts to define the minimal length of functional Vms1, we found that $Vms1^{11\text{-end}}$ is necessary and sufficient for full Vms1 function (Supplemental Figure S5A).

Direct, physical interaction between the Vms1 N-terminus and MTD

We hypothesized that the $Vms1^{MTD}$ targets Vms1 to mitochondria and that the N-terminal region ($Vms1^{1\text{-}182}$) acts to repress this targeting by direct interaction with the $Vms1^{MTD}$. Therefore $Vms1^{1\text{-}182}$ and $Vms1^{MTD}$ were tested for interaction, using multiple complementary methodologies. First, we generated yeast two-hybrid constructs expressing either $Vms1^{1\text{-}182}$ or $Vms1^{MTD}$ as a fusion with either the Gal4 DNA-binding domain (DBD) or activation domain (AD). In either orientation, the $Vms1^{1\text{-}182}$ and $Vms1^{MTD}$ fusions together enabled robust growth, indicating that these domains interact, similar to the positive control Alix/Tsg101 interaction (von Schwedler *et al.,* 2003), whereas none of the singly transformed fusions allowed growth (Figure 2A). To more rigorously test this interaction, we generated constructs expressing either $Vms1^{1\text{-}182}$ or $Vms1^{MTD}$ as a fusion with either the myc or hemagglutinin (HA) epitope tags. These constructs were expressed at physiological levels in a *vms1* mutant strain from the native *VMS1* promoter. We performed immunoprecipitation experiments on strains expressing the appropriate combinations of these constructs, as well as negative controls. As expected, the $Vms1^{1\text{-}182}$ and $Vms1^{MTD}$ domains exhibited a robust interaction in either orientation (Figure 2B). There was no evidence for either a $Vms1^{1\text{-}182}$–$Vms1^{1\text{-}182}$ or $Vms1^{MTD}$–$Vms1^{MTD}$ interaction, consistent with Vms1 being monomeric as observed by gel filtration chromatography.

$Vms1^{1\text{-}182}$ suppresses mitochondrial localization of $Vms1^{MTD}$

To further test the hypothesis that $Vms1^{1\text{-}182}$ prevents $Vms1^{MTD}$-mediated mitochondrial targeting, we overexpressed the $Vms1^{1\text{-}182}$

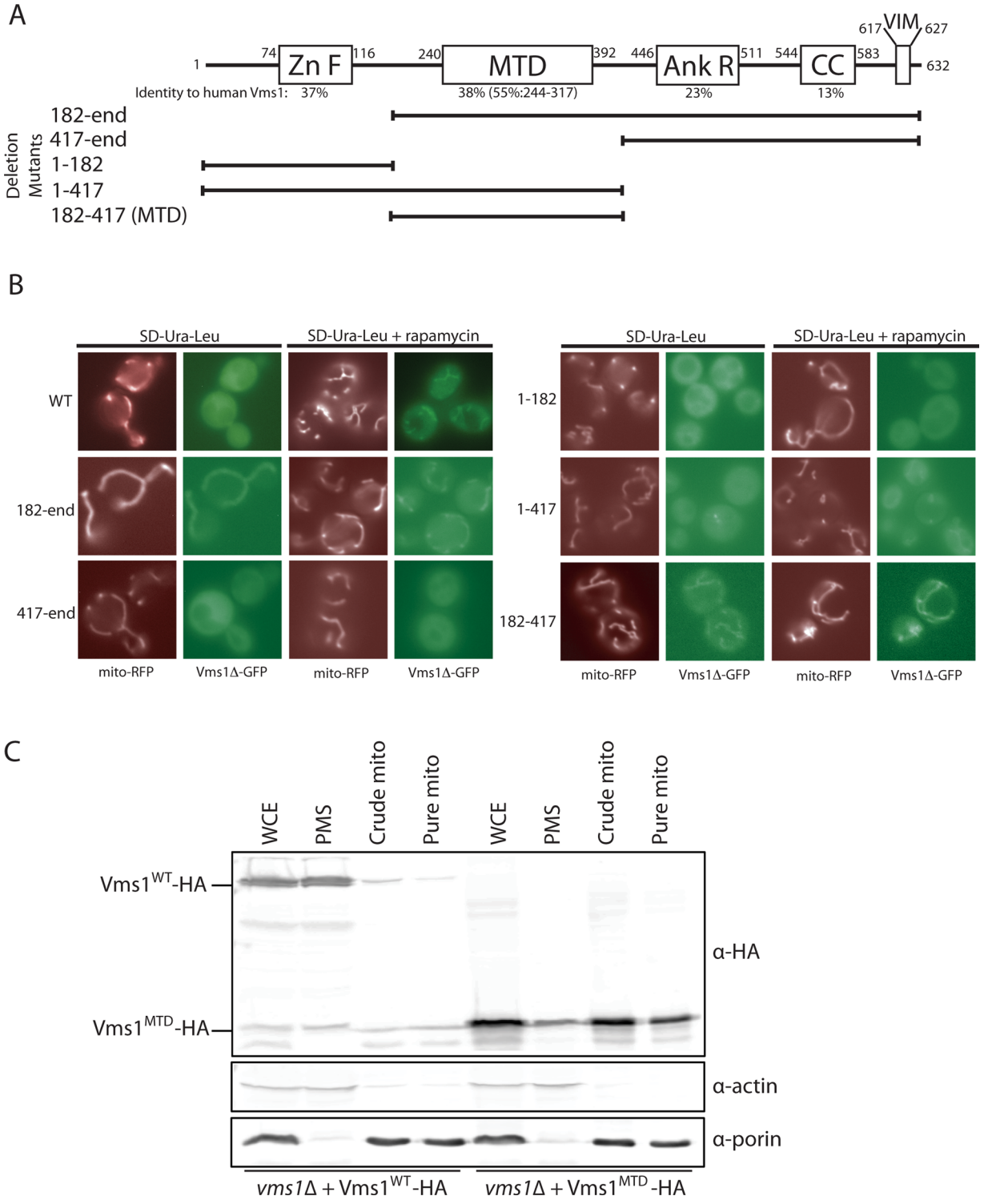

FIGURE 1: Mitochondrial localization of Vms1 requires the MTD and is inhibited by the N-terminus. (A) Schematic representation of the domain structure of full-length Vms1 and deletion mutants. Full-length Vms1 contains a ZnF, an MTD, an ankyrin repeat, a predicted coiled-coil region (CC), and a VIM. The percentage identity between *S. cerevisiae* and human Vms1 is indicated for each region. (B) The *vms1*Δ strain containing both a plasmid expressing mito-RFP and a plasmid expressing the indicated GFP-tagged Vms1 deletion mutant was grown in SD-Ura-Leu. On reaching mid–log phase, the culture was either treated with vehicle (left) or 200 ng/ml rapamycin (right) for 3 h. Note that the deletion mutants were expressed as C-terminal GFP fusions under control of the native *VMS1* promoter. Representative images are shown for each. (C) The *vms1*Δ mutant containing a plasmid expressing a C-terminus HA-epitope tagged full-length wild-type (cen) or MTD-only mutant ($Vms1^{MTD}$, 2μ) was grown in SGE-Ura medium. On reaching late log phase, cells were harvested and subjected to a mitochondrial isolation procedure as described. WCE, PMS, crude mitochondria (crude mito), and sucrose gradient–purified mitochondria (pure mito) were further analyzed for the presence of Vms1 by immunoblotting. Antibodies against actin (cytoplasm) or porin (mitochondria) were used to determine the purity of each fraction.

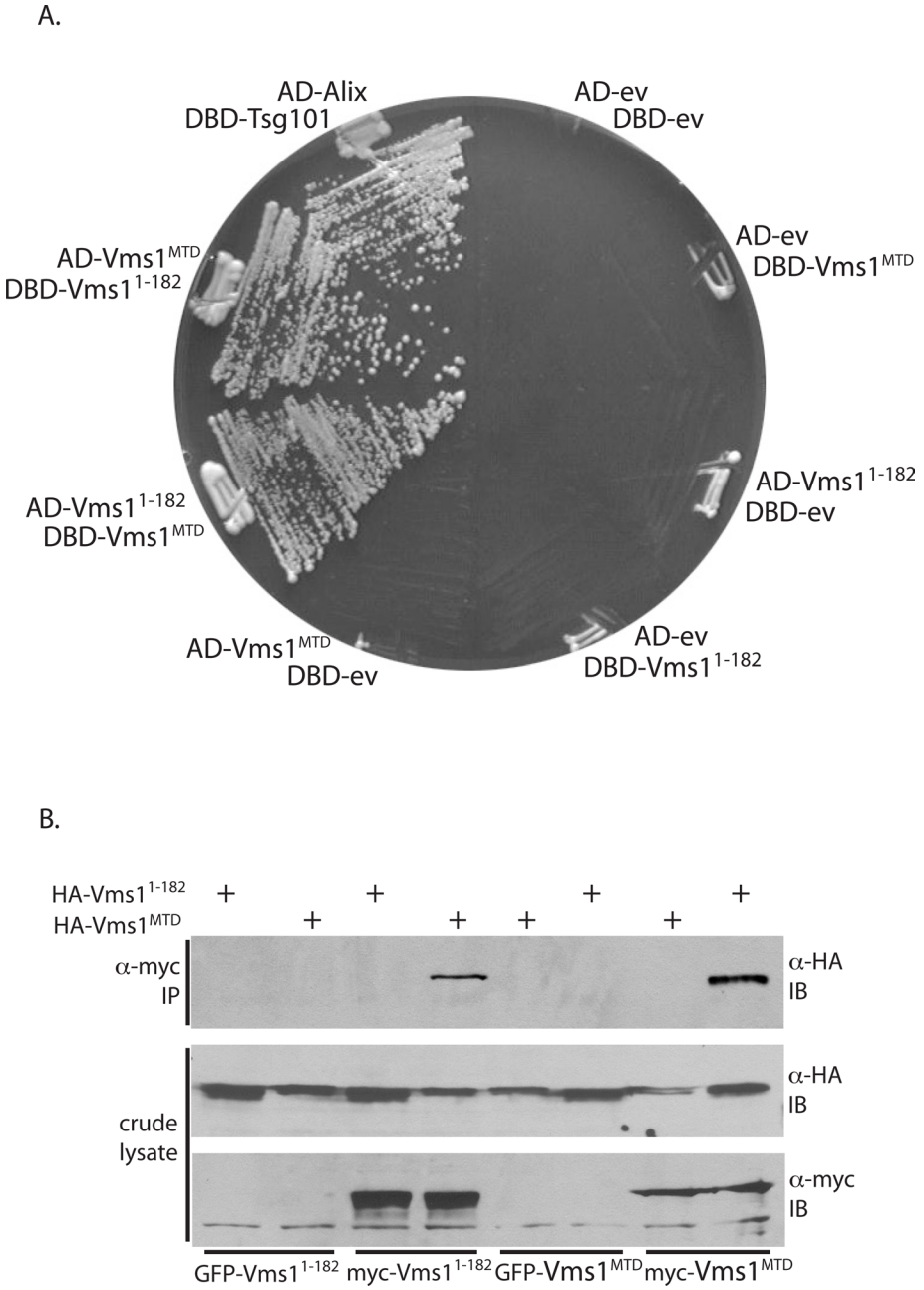

FIGURE 2: Vms1$^{1-182}$ and Vms1^{MTD} physically interact in vivo. (A) The AH109 strain was transformed with plasmids expressing AD and DBD fusions with nothing (ev), the Vms1$^{1-182}$, or the Vms1^{MTD}. AD-ALIX and DBD-TSG101 were used as a positive control. Each strain was streaked on an SD-Trp-Leu-His plate and grown at 30°C for 3 d. (B) For coimmunoprecipitation studies, the *vms1*Δ strain was transformed with plasmids encoding the Vms1$^{1-182}$ and Vms1^{MTD} tagged with GFP, myc, or HA as indicated, all under control of the native *VMS1* promoter. Each strain was grown to log phase in SD-Leu-Trp and harvested. The crude lysates from each strain were immunoprecipitated with anti-myc antibody, and Western blots were performed with anti-HA or anti-myc antibodies as indicated. Ten percent of crude lysate was loaded.

fragment in-*trans* with Vms1^{MTD} in yeast. This model would predict that overexpression of Vms1$^{1-182}$ might decrease the mitochondrial localization of Vms1^{MTD}. As observed previously, Vms1^{MTD} expressed on its own in a *vms1*Δ strain exhibited constitutive mitochondrial localization (Figures 1C and 3A). In contrast, upon overexpression of Vms1$^{1-182}$ under the galactose-inducible promoter, the majority of Vms1^{MTD} remained in the PMS, unbound to mitochondria (Figure 3A). As described previously, the Vms1^{MTD} appears to have a short half-life when expressed in isolation. Expression of the Vms1$^{1-182}$ fragment, however, significantly increased the levels of Vms1^{MTD}, presumably by delaying protein degradation. The increased steady-state accumulation of Vms1^{MTD} upon expression of Vms1$^{1-182}$ appears to be almost exclusively in the cytosol, consistent with the hypothesis that the N-terminal fragment is impeding mitochondrial localization of the MTD.

When we performed the same experiment using GFP-fused Vms1^{MTD} expressed from a low-copy centromeric plasmid, overexpression of Vms1$^{1-182}$ appeared to stabilize Vms1^{MTD}-GFP, as it was undetectable by immunoblotting without Vms1$^{1-182}$ expression (Figure 3B). Moreover, as in Figure 3A, most of the Vms1^{MTD} was observed in the cytosolic fraction, not associated with mitochondria. Taken together, these data are consistent with the hypothesis that the MTD domain targets Vms1 to mitochondria and the N-terminal 182 residues represses this targeting through direct interaction with the MTD.

The role of the N-terminus/MTD interaction in regulating Vms1 localization

To facilitate testing of the hypothesis that the N-terminus/MTD interaction regulates Vms1 translocation to mitochondria, we more precisely mapped the interacting regions in the Vms1$^{1-182}$ and Vms1^{MTD} fragments. Using the yeast two-hybrid system, we generated a series of deletion mutants (Supplemental Figure S3) and found that Vms1$^{11-55}$ was necessary and sufficient for the interaction with the Vms1^{MTD} (Figure 4A, right). Mapping of the interaction to this small region raised the possibility of generating full-length Vms1 variants in which the N-terminus/MTD interaction was disrupted by point mutations. Such mutants would enable us to rigorously evaluate our hypothesis that this interaction regulates Vms1 localization.

When we examined the sequence of Vms1$^{11-55}$ carefully, we found eight leucine residues located within this region that were disproportionately evolutionarily conserved (Figure 4B). When we aligned this Vms1 sequence with the consensus sequence for the leucine rich–repeat structural motif, LxxLxxN/CxL (x is any amino acid, and L can be replaced by valine, isoleucine, or phenylalanine), we observed significant but not complete homology. Leucine-rich repeats form an α/β horseshoe fold that is typically involved in mediating protein–protein interactions (Kobe and Kajava, 2001). To test whether these conserved leucines in Vms1 are indeed involved in the Vms1$^{11-55}$/Vms1^{MTD} interaction, we generated a mutant containing seven Leu-to-Ala mutations in Vms1$^{11-55}$ (MutA). This mutant did not interact with the Vms1^{MTD} in

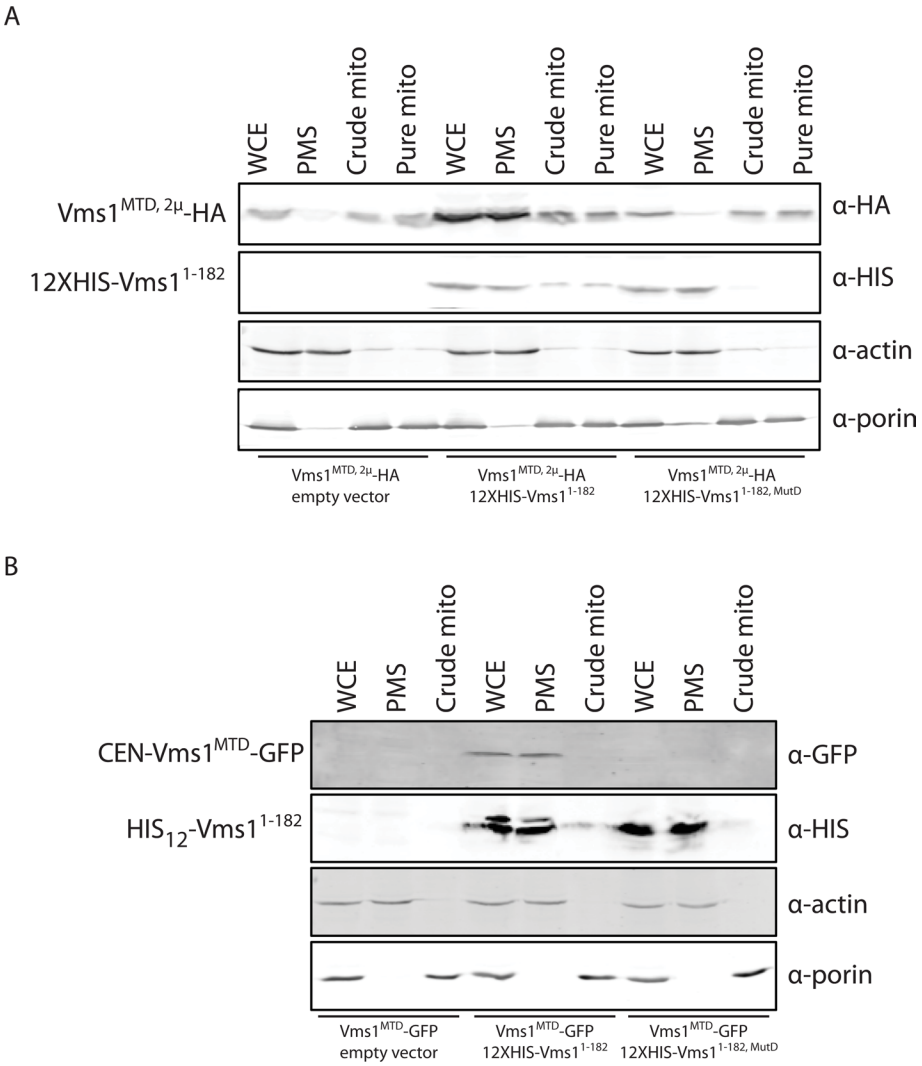

FIGURE 3: Overexpression of Vms1$^{1-182}$ stabilizes Vms1^{MTD} and sequesters it in the cytoplasm. (A) The JRY1734 strain (*pep4*::HIS3 *prb2*::LEU2 *bar1*::HISG *lys2*::GAL1/10-GAL4) was transformed with plasmids expressing C-terminally HA-tagged Vms1^{MTD} (2μ) and empty vector (ev), N-terminally His$_{12}$-tagged Vms1$^{1-182}$, or Vms1$^{1-182, MutD}$. Each strain was grown in SGE-Ura-Trp media at 30°C. On reaching mid–log phase, galactose was added to a final concentration of 0.4%. After additional growth for 4 h, cells were harvested and subjected to mitochondrial isolation as described. Representative images of three independent experiments are shown. (B) Same set of experiments as in A, performed using C-terminally GFP-fused Vms1^{MTD} expressed under the *VMS1* promoter rather than the HA-tagged Vms1^{MTD} (2μ).

the yeast two-hybrid assay, and introduction of these mutations in full-length Vms1 caused constitutive mitochondrial localization of Vms1 (Supplemental Figure S4). These data are consistent with our hypothesis that these leucine residues play a critical role in the formation of the N-terminus/MTD interaction and this interaction represses mitochondrial localization of Vms1. The MutA mutant of Vms1 failed to rescue the rapamycin hypersensitivity of the *vms1*Δ mutant (Supplemental Figure S5A). This is probably due to its instability and decreased steady-state levels, especially in cells treated with rapamycin (Supplemental Figure S5B).

We generated Vms1 variants in which a subset of the MutA residues were mutated to attempt to disrupt the N-terminus/MTD interaction while maintaining better protein stability (Figure 4B). We also included mutations targeting other highly conserved residues in this region. Among three new mutants generated, one of them (MutB) did not impair interaction with the MTD. The two others (MutC and MutD), however, no longer interacted with the MTD in the yeast two-hybrid assay (Figure 4A, right). We then introduced these mutations into HA-tagged Vms1$^{1-182}$ and performed coimmunoprecipitation experiments with myc-tagged Vms1^{MTD}. As shown in Figure 4C, the MutC mutant exhibited impaired MTD interaction, and the MTD interaction was completely lost in the MutD mutant.

To test the hypothesis that the N-terminus/MTD interaction regulates Vms1 localization, we generated a full-length version of Vms1 bearing the MutD mutations (Leu^{23}Leu^{28}Leu^{31}Leu^{33} to Ala^{23}Ala^{28}Ala^{31}Ala^{33}), which completely disrupts this interaction. Before testing the effect of MutD on Vms1 localization, we first assessed the functionality of this construct by ability to rescue a *vms1*Δ mutant. Unlike Vms1^{MutA} mentioned before, full-length Vms1^{MutD} was similarly functional to wild-type Vms1 (Supplemental Figure S6). Although Vms1^{MutD} steady-state accumulation was not at the level of wild-type Vms1, it was significantly higher than Vms1^{MutA} (Supplemental Figure S5B). We then examined the effect of these mutations on Vms1 localization by expressing C-terminally GFP-tagged, full-length Vms1^{MutD} in the *vms1* mutant. As before, wild-type Vms1 was cytoplasmic under normal conditions without any stressor (Figure 5A, top). Full-length Vms1^{MutD}, however, exhibited increased mitochondrial localization compared with the wild type (Figure 5A, bottom). To further test this enhanced mitochondrial localization of Vms1, we performed biochemical fractionation of cells expressing HA-tagged full-length wild-type Vms1 or Vms1^{MutD}. In agreement with the fluorescence localization, we observed increased Vms1^{MutD} levels in purified mitochondria even after sucrose gradient purification of crude mitochondria in normal conditions (Figure 5B).

Previously we showed that overexpression of Vms1$^{1-182}$ stabilizes and sequesters Vms1^{MTD} in the cytoplasm (Figure 3, A and B). If these effects are dependent on the N-terminus/MTD interaction, overexpression of the Vms1$^{1-182, MutD}$ variant should be ineffective. As expected, overexpression of the MutD variant had no effect on either MTD stability and expression level or on its mitochondrial localization (Figure 3, A and B). These data suggest that the N-terminus/MTD interaction maintains Vms1 in the cytoplasm, whereas dissociation leads to mitochondrial translocation of Vms1.

Vms1-centric regulatory signals controlling Vms1 localization

The foregoing observations encouraged us to attempt to identify the stimuli and mechanisms that regulate the N-terminus/MTD interaction. One possible scenario is a change in posttranslational modification(s) of Vms1 upon stress stimuli. We performed

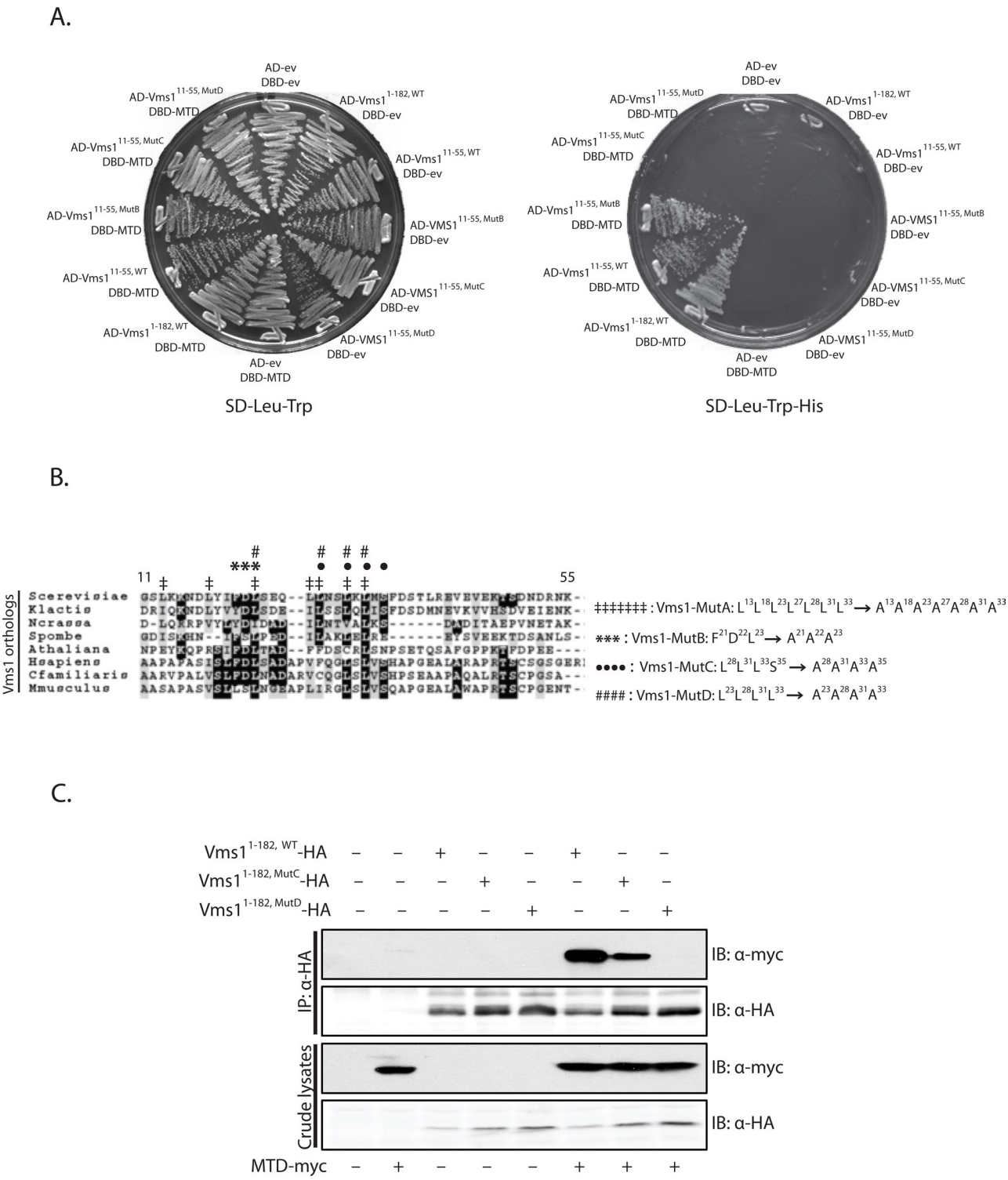

FIGURE 4: Vms1$^{11\text{-}55}$ is necessary and sufficient for interaction with Vms1^{MTD}. (A) The AH109 strain was transformed with plasmids expressing AD and DBD fusions with nothing (ev), Vms1$^{11\text{-}55}$, Vms1^{MutB}, Vms1^{MutC}, Vms1^{MutD}, or Vms1^{MTD}. AD-Vms1$^{1\text{-}182}$ and DBD-Vms1^{MTD} were used as a positive control. Each strain was streaked on both SD-Trp-Leu (left, control) and SD-Trp-Leu-His (right) plates and grown at 30°C for 3 d. (B) Sequence alignment of Vms1$^{11\text{-}55}$ among *VMS1* orthologues from other species. (C) For coimmunoprecipitation studies, the *vms1*Δ strain was transformed with plasmids encoding Vms1$^{1\text{-}182}$, Vms1$^{1\text{-}182,\ MutC}$, Vms1$^{1\text{-}182,\ MutD}$, and Vms1^{MTD} tagged with myc or HA as indicated, all under control of the native *VMS1* promoter. Each strain was grown to log phase in SD-Leu-Trp and harvested. The crude lysates from each strain were immunoprecipitated with anti-HA antibody, and Western blots were performed with anti-HA or anti-myc antibodies as indicated. Ten percent of crude lysate was loaded.

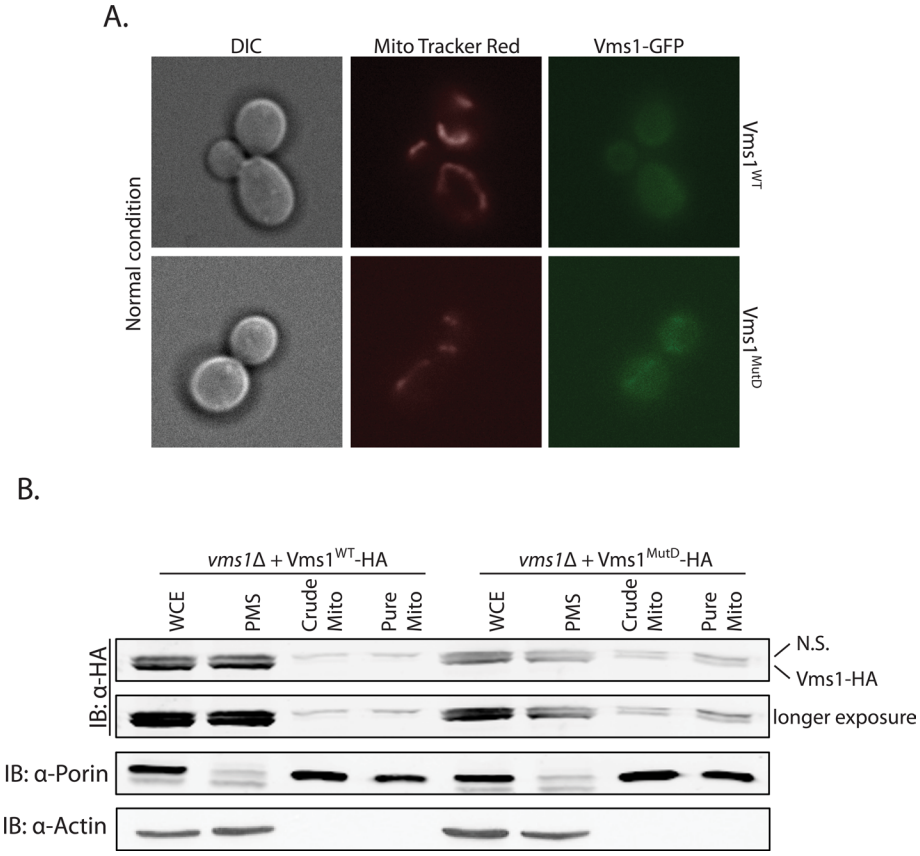

FIGURE 5: Disruption of the Vms1 intramolecular interaction facilitates mitochondrial translocation of Vms1. (A) The *vms1*Δ strain containing a plasmid expressing GFP-tagged wild-type Vms1 or Vms1^{MutD} was grown in SD-Ura medium. On reaching log phase, cells were subjected to fluorescence microscopy to detect Vms1 localization. Representative images are shown. (B) The *vms1*Δ strain containing a plasmid expressing HA-tagged wild-type Vms1 or Vms1^{MutD} was grown in SD-Ura and harvested at log phase. Cells were then subjected to mitochondrial isolation and subsequent sucrose gradient purification. The same fraction of each sample was subjected to SDS–PAGE and subsequent Western blot. Antibodies against actin (cytoplasm) or porin (mitochondria) were used to determine the purity of each fraction. Representative images of three independent experiments are shown.

comprehensive proteomic profiling of Vms1 in the presence and absence of rapamycin, which robustly induces mitochondrial translocation. We mapped four serine and threonine residues located within the Vms1$^{1-182}$ fragment exhibiting approximately a twofold reduction in phosphorylation levels upon rapamycin treatment, raising the possibility that dephosphorylation might facilitate dissociation from the MTD and mitochondrial localization of Vms1 (Supplemental Figure S7A). Therefore we mutated all of these residues to alanine to mimic the fully dephosphorylated state and performed coimmunoprecipitation assays, as well as fluorescence imaging. These alanine mutations had no effect on the interaction with the Vms1^{MTD} compared with the wild-type Vms1$^{1-182}$. Neither did this mutant exhibit any change in subcellular localization relative to the wild-type control (Supplemental Figure S7, B and C). Mutation of these sites to glutamate also had no effect on Vms1^{MTD} interaction or localization. Therefore, although phosphorylation of these residues within the Vms1 N-terminus might play a role in regulating Vms1 function, it appears to be neither necessary nor sufficient to control Vms1 localization. Zinc binding to the N-terminal zinc finger domain also is not required, as mutation of the two obligate cysteine residues had no effect on Vms1 localization.

Selective Vms1 recruitment to damaged mitochondria

The failure to find Vms1-focused regulatory events that were required for stress-responsive translocation to mitochondria raised the possibility that Vms1 localization might be controlled by modification of mitochondria rather than modification of Vms1. To approach this issue, we sought to determine the location of the mitochondrial stress "signal." Does the presence of mitochondrial stress cause a generalized recruitment of Vms1 to mitochondria across the entire cell? Alternatively, are damaged mitochondria selectively marked such that they are specifically targeted for Vms1 localization? To enable localized oxidative damage of mitochondria, we utilized mitochondrially targeted KillerRed (mito-KillerRed; Bulina *et al.*, 2006; Shibuya and Tsujimoto, 2012). KillerRed is a mutated form of red fluorescent protein (RFP; anm2CP) from the hydrozoan Anthomedusae that generates the reactive oxygen species (ROS) singlet oxygen and superoxide upon irradiation with green light (Bulina *et al.*, 2006). To first determine whether mitochondrial ROS induced by KillerRed irradiation was sufficient to induce Vms1 translocation to mitochondria, we irradiated entire fields of cells and monitored Vms1-GFP localization over time. By 30 min postirradiation, we observed colocalization of Vms1-GFP with mitochondria, which became maximal at approximately 1 h (Figure 6A). Conversely, Vms1-GFP showed no mitochondrial localization upon irradiation in cells expressing mitochondrial-targeted RFP that does not emit ROS (Supplemental Figure S8). It is important to note that the photobleaching of the KillerRed fluorescence that we observed is an expected indication of its photoactivation (Bulina *et al.*, 2006) and that KillerRed activation seems to modestly promote mitochondrial fragmentation but has little effect on mitochondrial position during the 60-min time course. We also verified that the observed GFP localization at mitochondria was specific for Vms1-GFP, as cells expressing KillerRed alone did not show GFP localization under identical exposure conditions (Supplemental Figure S9).

Having verified that KillerRed activation induced Vms1 localization to mitochondria, we then focally irradiated only a subset of mitochondria within cells and examined Vms1-GFP localization. As shown in Figure 6B and Supplemental Figure S10, localized irradiation with green light caused cytosolic depletion of Vms1-GFP and preferential recruitment of Vms1 specifically to those mitochondria activated for superoxide generation. Quantification of many similar images ($n = 105$) showed an increase in Vms1-GFP localization at the site of irradiated mitochondria (Figure 6C). This was accompanied by a depletion of cytosolic Vms1-GFP (Figure 6C), consistent with recruitment of cytosolic Vms1 to irradiated mitochondria. The levels of Vms1 at mitochondria distal to the site of irradiation were unchanged by irradiation (Figure 6C). Taken together, these results suggest that damaged mitochondria display a signal(s) that facilitates specific Vms1 recruitment.

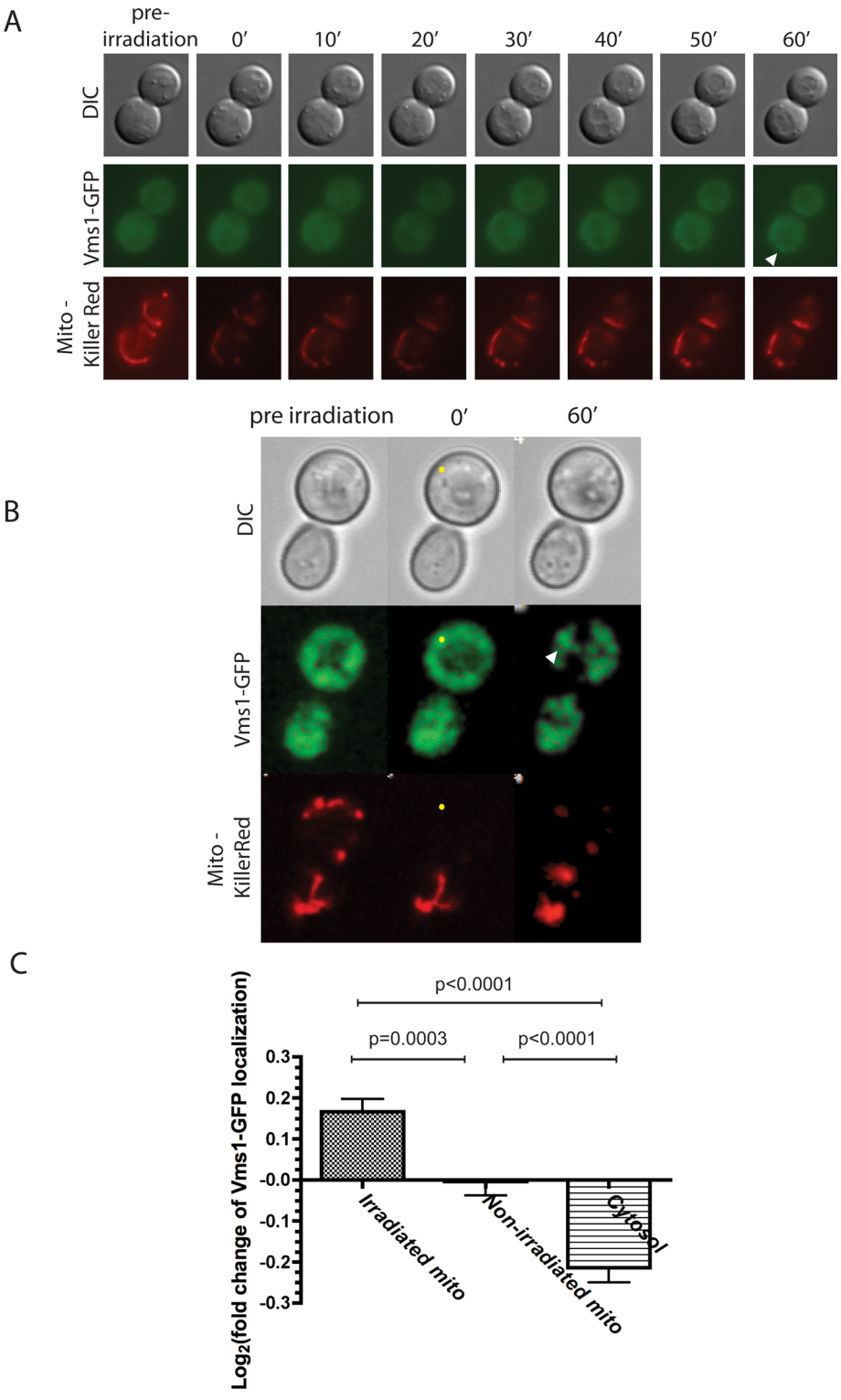

FIGURE 6: Vms1 exhibits preferential localization to ROS-exposed mitochondria. (A) Yeast cells expressing Vms1-GFP were transformed with a mitochondrially targeted KillerRed, which generates superoxide and singlet oxygen upon irradiation with green light. Cells were irradiated for 15 min with 572-nm light. After irradiation, Vms1-GFP localization was monitored by wide-field fluorescence microscopy every 10 min for 60 min. (B) The cells described were irradiated with a 543-nm HeNe laser at 100% intensity for 1 min and only in a small region of the cell (indicated by the yellow dot), which contained mitochondria. Vms1-GFP localization was monitored by confocal fluorescence microscopy for 60 min after irradiation. (C) Quantification of Vms1-GFP localization to irradiated mitochondria, nonirradiated mitochondria, and the cytosol is shown as described in *Materials and Methods*.

DISCUSSION

Here we described a regulatory mechanism for Vms1 localization. In wild-type cells maintained in normal laboratory conditions, Vms1 was cytosolic, but in response to a variety of stress stimuli, Vms1 translocated to mitochondria (Heo *et al.*, 2010). We found that the MTD region of Vms1 is necessary and sufficient for mitochondrial localization. This is the most highly conserved region among Vms1 orthologues but has no significant similarity to any protein outside of the Vms1 family (Supplemental Figure S1). In particular, the N-terminal 70 amino acids of this region are ~50% identical among the major eukaryotic *VMS1* orthologues. It is tempting to speculate that this level of conservation implies a mechanism for Vms1 mitochondrial targeting that is distinct from a simple protein–protein interaction. Resolving this question will most likely require the structure of the Vms1 protein and/or identification of a specific mitochondrial receptor of Vms1.

Our biochemical fractionation and in vivo imaging studies demonstrate that the mitochondrial targeting activity of the MTD is repressed by the Vms1 N-terminus, probably through direct physical association. On discovering this interaction, we hypothesized that the interaction between $Vms1^{1\text{-}182}$ and $Vms1^{MTD}$ might be disrupted in response to mitochondrial stress stimuli, such as rapamycin, allowing the MTD to target Vms1 to mitochondria. In turn, Vms1 would recruit Cdc48 and Npl4 to mitochondria to carry out proteasomal degradation. Attempts to directly test whether the $Vms1^{1\text{-}182}$ and $Vms1^{MTD}$ interaction is disrupted by mitochondrial stress failed, in both coimmunoprecipitation and two-hybrid experiments, due to technical problems with these systems. We were able to test the importance of this interaction in Vms1 localization, however, using a mutant incapable of forming the $Vms1^{1\text{-}182}$/$Vms1^{MTD}$ interaction. If the model is correct, disruption of this interaction should increase the levels of mitochondrially localized Vms1. Indeed, when we introduced mutations that impair the interaction in full-length Vms1, we observed elevated levels of mitochondrial Vms1 in both imaging and biochemical fractionation studies. Although we were unable to demonstrate regulated dissociation of this interaction in vivo under physiological conditions, we demonstrated that dissociation of this interaction by mutations liberates the MTD, which is sufficient to target Vms1 to mitochondria. We believe it is likely that the N-terminus/MTD interaction is intramolecular, as we saw no evidence of Vms1

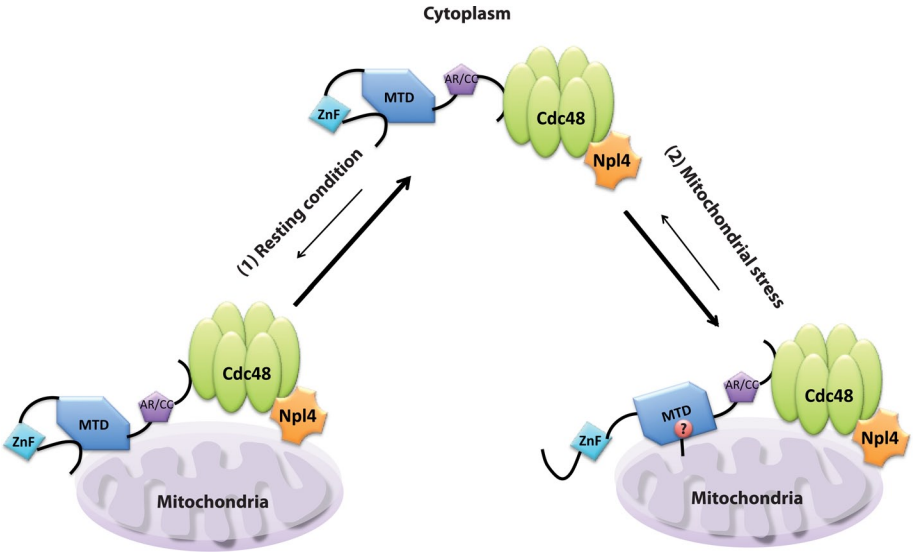

FIGURE 7: Intramolecular interactions regulate Vms1 localization to mitochondria. In resting and unstressed conditions, Vms1 is maintained in the cytosol through a stable intramolecular interaction between residues 1–182 and the MTD. Under stress conditions, specifically those conditions that necessitate the recruitment of the ubiquitin/proteasome system to mitochondria, a mitochondrial damage signal accumulates. Vms1 binds to mitochondria possessing this signal, which further promotes the disruption of the intramolecular interaction between residues 1–182 and the MTD, enabling a stable MTD/mitochondrial interaction.

oligomerization, but we cannot rule out the possibility that the N-terminus of one molecule of Vms1 can bind to and repress the mitochondrial localization of another molecule.

We observed that interaction with the N-terminus not only prevents mitochondrial localization of the MTD, but also stabilizes it. As shown in our biochemical fractionation experiments, overexpression of Vms1$^{1\text{-}182}$ increased the Vms1^{MTD} protein level, whereas Vms1$^{1\text{-}182,MutD}$ did not. Consistent with these data, Vms1$^{1\text{-}417,\ MutD}$ lacking this intramolecular interaction was unstable when expressed either in *Escherichia coli* or in yeast (J.M.H. and J.R., unpublished data). We therefore predict that the formation of this Vms1 intramolecular interaction protects Vms1^{MTD} from the exposure of hydrophobic and/or disordered regions to maintain a state that is latent but competent. On mitochondrial stress, however, this interaction is disrupted, which, in turn, facilitates mitochondrial targeting of the exposed Vms1^{MTD}. This is consistent with our observations that rapamycin and other stress conditions lead to reduced levels of Vms1, presumably a result of this active and unstable conformation.

One major remaining question relates to the nature of the signal that regulates the stability of the N-terminus/MTD interaction and thereby regulates mitochondrial localization. One possibility is the presence of protein(s) that interact with either the N-terminus or the MTD to modulate their affinity for one another. However, we have not observed such protein(s) preferentially bound to Vms1 in either the presence or absence of rapamycin treatment in our biochemical purification experiments. The second possible scenario is a change in posttranslational modification(s) on Vms1 upon stress stimuli. Although we found four sites of phosphorylation located within the Vms1$^{1\text{-}182}$ fragment that exhibit roughly twofold reduced levels of phosphorylation upon rapamycin treatment, our mutagenesis studies showed that phosphorylation of these sites was neither necessary nor sufficient to promote Vms1 translocation.

This led us to consider alternative regulatory mechanisms by which extrinsic factor(s) might regulate Vms1 localization. Perhaps the signal leading to disruption of the Vms1 intramolecular interaction was not affecting Vms1 directly but was instead localized to the Vms1^{MTD} target site, specifically mitochondria. We therefore reasoned that damaged mitochondria might harbor a recruitment signal for Vms1. This hypothesis was tested using mitochondrial KillerRed, which generates light-induced reactive oxygen species within the mitochondrial matrix. On a whole-cell level, irradiation caused mitochondrial localization of Vms1. More importantly, activation of mitochondrial KillerRed within a subset of mitochondria caused preferential localization of cytosolic Vms1 specifically to that subpopulation without affecting Vms1 localization to nonirradiated mitochondria. Although this effect is highly statistically significant when quantified over a large number of replicates, the magnitude of the effect is rather modest. We suggest that the scale of the observed effect is likely to be an underrepresentation of the selectivity of mitochondrial recruitment in more physiological situations. This is due to the experimental complexities inherent in this paradigm, including the spatially imprecise irradiation on our microscope system and the movement within cells of reactive oxygen species and their products. Both of these limitations tend to decrease the apparent spatial specificity of Vms1 recruitment. In spite of these challenges, this observation has important implications for the nature of the signal promoting Vms1 translocation. Although its identity remains unclear, that signal appears to specifically mark damaged mitochondria and promote the recruitment of cytosolic Vms1. This could have important implications for pathological situations that are characterized by the presence of mitochondrial damage or stress.

These data suggest that both the N-terminus/MTD interaction and a signal localized to damaged mitochondria play important roles in regulating Vms1 localization within the cell. We hypothesize that their functions are interrelated. One possible explanation is that a stress-responsive accumulation of one or more specific mitochondrial modifications (one possibility being ubiquitin conjugates) competes with the Vms1$^{1\text{-}182}$/Vms1^{MTD} interaction. In this model (Figure 7), the Vms1$^{1\text{-}182}$/Vms1^{MTD} interaction is stable in normal conditions, and this represses mitochondrial translocation. Under stress conditions, specifically those conditions that necessitate the recruitment of the ubiquitin/proteasome system to mitochondria, the mitochondrial damage signal is accumulated. Cytosolic Vms1 binds to mitochondria possessing this signal, which then further promotes the open conformation, enabling a stable MTD/mitochondrial interaction.

The mitochondrial localization of the damage signal has interesting implications. Under stress conditions, those mitochondria that are spared from damage are also spared from Vms1 recruitment. This marking system enables the specific recruitment of the machinery to the sites where it is most needed. An analogous marking system appears to be operative under the more extreme case in which mitochondria are targeted for total degradation by autophagy (Youle and Narendra, 2011). Perhaps these two degradative systems are part of a continuum in which attempts are first made to rescue mitochondrial function through targeted protein degradation. If that

fails to restore mitochondrial bioenergetics, the entire organelle is then destroyed through autophagy.

Many lines of evidence suggested the existence of communication between mitochondria and other organelles, including the nucleus and endoplasmic reticulum. In this study, we provide an additional line of evidence that mitochondria communicate a damage signal to the cytosol. Although further studies are necessary to define this mitochondrial-derived signal, it is clear that the cellular stress-response machinery, including the Vms1 system, recognizes this signal and acts to protect and repair mitochondria. The result is the maintenance of mitochondrial function under challenging conditions, which is necessary for cell and organismal viability.

MATERIALS AND METHODS

Yeast strains, media, and growth conditions

A W303a *Saccharomyces cerevisiae* strain (W303a *MATa his3 leu2 met15 trp1 ura3*) was used as the parental and wild-type strain. Deletion mutant strains were generated by standard PCR-based homologous recombination methods in diploids, followed by sporulation and tetrad dissection. Yeast were transformed by the lithium acetate method and grown at 30°C in SD medium (0.67% yeast nitrogen base, 2% glucose) with amino acids unless otherwise indicated (Sherman, 1991).

Plasmid construction

Plasmids expressing C-terminally HA- and GFP-tagged Vms1 were generated as described (Heo *et al.,* 2010). The *VMS1* coding region and promoter was PCR amplified from genomic DNA and ligated in-frame into a pRS416-based vector containing a C-terminal HA_3 or GFP tag. *VMS1* deletion mutant constructs were PCR amplified from the *VMS1* coding region corresponding to 544nt-end, 1249nt-end, 1-546nt, 1-1251nt, and 544nt-1251nt, respectively. These fragments were ligated in-frame into a pRS416-based vector flanked by the endogenous *VMS1* promoter and C-terminal GFP.

For constructs used in $Vms1^{1\text{-}182}$ and $Vms1^{MTD}$ coimmunoprecipitation, regions corresponding to mutant 1-182 ($Vms1^{1\text{-}182}$) and mutant 182-417 ($Vms1^{MTD}$) were PCR amplified and ligated in-frame into a pRS416-based vector containing the endogenous *VMS1* promoter and a C-terminal HA_3 (or Myc_{13}) tag.

For constructs with mutations, the sewing PCR strategy was used. PCR-amplified *VMS1* with mutations was ligated into the identical vector systems used for wild-type Vms1.

Fluorescence microscopy

The *vms1*Δ strain was transformed with both pVMS1-GFP (or pVMS1 deletion mutant-GFP) and pMito-RFP plasmids. To test the effect of rapamycin treatment on Vms1 localization, strains were grown to log phase at 30°C in SD medium lacking both uracil and leucine, treated with vehicle or rapamycin (200 ng/ml) for 3 h, and imaged using a Zeiss Axioplan 2 Imaging microscope (Carl Zeiss, Jena, Germany) as described (Kondo-Okamoto *et al.,* 2003). To test the localization of Vms1 mutant in normal conditions without any stressor treatment, the *vms1*Δ strain transformed with indicated Vms1 mutant was grown to log phase at 30°C in SD-Ura medium, stained with Mitotracker Red dye (Invitrogen, Carlsbad, CA), and subjected to imaging as described.

For Mitotracker Red staining, 200 μl of individual cultures were stained with 10 μl of 10 μM MitoFluor Red 589 (Molecular Probes, Eugene, OR) for a couple of seconds and washed three times with the same volume of media. Cells were then subjected to fluorescence microscopy as described.

Mitochondrial isolation

Cells were harvested at the indicated time point and subjected to mitochondrial preparation as previously described (Hao *et al.,* 2009). Isolated mitochondria were further purified by sucrose gradient purification as described (Heo *et al.,* 2010).

Yeast two-hybrid system

The yeast two-hybrid assay was performed following the manufacturer's guidelines (Matchmaker Two-Hybrid System 3; Clontech, Mountain View, CA). The AH109 strain (*MATa, trp1-901, leu2-3, 112, ura3-52, his3-200, gal4*Δ, *gal80*Δ, *LYS2 : : $GAL1_{UAS}$-$GAL1_{TATA}$-HIS3, $GAL2_{UAS}$-$GAL2_{TATA}$-ADE2, URA3 : : $MEL1_{UAS}$-MEL1 $_{TATA}$-lacZ*) was transformed with various combinations of pGBKT7- and pGADT7-based constructs harboring no insert, $Vms1^{1\text{-}182}$, $Vms^{11\text{-}55}$, $Vms^{11\text{-}55,\ MutA}$, $Vms1^{11\text{-}55,\ MutB}$, $Vms1^{11\text{-}55,\ MutC}$, $Vms1^{MTD}$, or positive controls. These strains were then streaked on SD-Leu-Trp-His plates to test for growth, which was indicative of an interaction.

Immunoprecipitation

$Vms1^{1\text{-}182}$ and $Vms1^{MTD}$ coimmunoprecipitation was performed as described (Hayden and Ghosh, 2008). The *vms1*Δ strain transformed with the indicated combinations of constructs was grown to log phase, harvested, resuspended, and lysed in solution A (50 mM Tris-HCl, pH 7.4, 50 mM NaCl, 0.2% Triton X-100, and protease inhibitor cocktails [Sigma-Aldrich, St. Louis, MO]). Cleared lysates were incubated with anti-Myc (Sigma-Aldrich) or anti-HA antibody (Covance, Berkeley, CA) for 1 h at 4°C, followed by incubation with recombinant protein G beads for 1 h at 4°C. After washing, bound proteins were eluted in SDS, separated by SDS–PAGE, and applied to Western blotting using anti-HA or -myc antibodies as indicated. Ten percent of crude lysates was loaded.

Vms1 purification in yeast

Yeast strain JRY1734 (*pep4*::HIS3 *prb2*::LEU2 *bar1*::HISG *lys2*::GAL1/10-GAL4), designed for efficient overexpression, was transformed with a plasmid expressing N-terminus His_{12}-fused $Vms1^{1\text{-}417}$ under the galactose-inducible promoter as described (von Schwedler *et al.*, 2003). Transformed cells were grown to mid–log phase in SGlycerol (3%) ethanol (2%)–Ura medium. To induce the expression of Vms1, galactose was added to the final concentration of 0.2%, and cells were grown for an additional 4 h and harvested. To purify Vms1, cells were lysed and subjected to conventional nickel affinity purification using nickel-nitriloacetic acid beads and following the protocol suggested by the vendor (Fisher Scientific, Pittsburgh, PA).

Mito-Killer irradiation and Vms1 localization

A strain expressing Vms1-GFP from the *VMS1* locus (VMS1::VMS1-GFP-HIS3MX) yeast cells was transformed with a plasmid encoding a GPD promoter–driven construct expressing Killer Red (Evrogen, Moscow, Russia) fused with the mitochondrial targeting sequence of Su9 in a pRS415 backbone. These cells were grown to log phase in SD medium lacking leucine and imaged using a Zeiss Axioplan 2 Imaging microscope after 15 min of irradiation with 572-nm green light from an X-Cite Series 120 fluorescence lamp. In experiments requiring irradiation of a portion of the mitochondria, these cells were irradiated with a 543-nm-wavelength HeNe laser (100% intensity) for 1 min and imaged with a FV1000XY Confocal IX81 microscope (Olympus, Tokyo, Japan; University of Utah Fluorescence Microscopy Facility, Salt Lake City, UT).

To quantify Vms1-GFP localization, the average fluorescence intensity was measured (Image J; National Institutes of Health,

Bethesda, MD) from images taken before and 60 min postirradiation in three regions of equal area: a region of irradiated mitochondria, a region of nonirradiated mitochondria, and a cytosolic region lacking mitochondria. The average fluorescence intensity in the whole cell was also measured from images taken before and 60 min postirradiation. The ratio of postirradiation to preirradiation fluorescence intensity for each of the three regions was calculated and normalized to the postirradiation:preirradiation ratio of average total cellular intensity in order to account for any photobleaching effects.

ACKNOWLEDGMENTS

We thank Tim Formosa for yeast strains and helpful advice, Don Ayer for the anti-His antibody, Wes Sundquist for the yeast two-hybrid system vectors and strain, Chris Rodesch for assistance with fluorescence microscopy, and Brad Cairns for use of the yeast pulverizer. We also thank the Rutter lab for helpful advice and suggestions. This work was supported by National Institutes of Health Grant GM087346 (J.R.).

REFERENCES

Bulina ME, Chudakov DM, Britanova OV, Yanushevich YG, Staroverov DB, Chepurnykh TV, Merzlyak EM, Shkrob MA, Lukyanov S, Lukyanov KA (2006). A genetically encoded photosensitizer. Nat Biotechnol 24, 95–99.

Calvo SE, Mootha VK (2010). The mitochondrial proteome and human disease. Annu Rev Genomics Hum Genet 11, 25–44.

Chan NC, Salazar AM, Pham AH, Sweredoski MJ, Kolawa NJ, Graham RL, Hess S, Chan DC (2011). Broad activation of the ubiquitin-proteasome system by Parkin is critical for mitophagy. Hum Mol Genet 20, 1726–1737.

Hao HX *et al.* (2009). SDH5, a gene required for flavination of succinate dehydrogenase, is mutated in paraganglioma. Science 325, 1139–1142.

Hayden MS, Ghosh S (2008). Shared principles in NF-kappaB signaling. Cell 132, 344–362.

Heo JM *et al.* (2010). A stress-responsive system for mitochondrial protein degradation. Mol Cell 40, 465–480.

Heo JM, Rutter J (2011). Ubiquitin-dependent mitochondrial protein degradation. Int J Biochem Cell Biol 43, 1422–1426.

Kissová I, Deffieua M, Samokhvalova V, Veloursa G, Bessoulec J, Manona S, Camougrand N (2006). Lipid oxidation and autophagy in yeast. Free Radic Biol Med 41, 1655–1661.

Kobe B, Kajava AV (2001). The leucine-rich repeat as a protein recognition motif. Curr Opin Struct Biol 11, 725–732.

Kondo-Okamoto N, Shaw JM, Okamoto K (2003). Mmm1p spans both the outer and inner mitochondrial membranes and contains distinct domains for targeting and foci formation. J Biol Chem 278, 48997–49005.

Lin MT, Beal MF (2006). Mitochondrial dysfunction and oxidative stress in neurodegenerative diseases. Nature 443, 787–795.

Livnat-Levanon N, Glickman MH (2011). Ubiquitin-proteasome system and mitochondria—reciprocity. Biochim Biophys Acta 1809, 80–87.

Pan Y (2011). Mitochondria, reactive oxygen species, and chronological aging: a message from yeast. Exp Gerontol 46, 847–52.

Sherman F (1991). Getting started with yeast. In: Guide to Yeast Genetics and Molecular Biology, ed. C Guthrie and GR Fink, San Diego, CA: Academic Press, 3–21.

Sickmann A *et al.* (2003). The proteome of *Saccharomyces cerevisiae* mitochondria. Proc Natl Acad Sci USA 100, 13207–13212.

Shibuya T, Tsujimoto Y (2012). Deleterious effects of mitochondrial ROS generated by KillerRed photodynamic action in human cell lines and C. elegans. J Photochem Photobiol B 117, 1–12.

Tanaka A, Cleland MM, Xu S, Narendra DP, Suen DF, Karbowski M, Youle RJ (2010). Proteasome and p97 mediate mitophagy and degradation of mitofusins induced by Parkin. J Cell Biol 191, 1367–1380.

von Schwedler UK *et al.* (2003). The protein network of HIV budding. Cell 114, 701–713.

Xu S, Peng G, Wang Y, Fang S, Karbowski M (2011). The AAA-ATPase p97 is essential for outer mitochondrial membrane protein turnover. Mol Biol Cell 22, 291–300.

Youle RJ, Narendra DP (2011). Mechanisms of mitophagy. Nat Rev Mol Cell Biol 12, 9–14.